IMAGE ANALYSES CHARACTERIZATION OF THE MICROSTRUCTURE IN DUCTILE IRON (*)

Edvaldo C. Angelo Jr
Pontifícia Universidade Católica do Paraná, Imaculada Conceição St, 1155, Prado Velho, Zip Code 80215-901, Department of Mechanical Engineering, Curitiba, Paraná, Brazil, Tel. 55 41 330-1346.
e-mail: e_angelo@hotmail.com.

Ricardo D. Torres
Pontifícia Universidade Católica do Paraná, Imaculada Conceição St, 1155, Prado Velho, Zip Code 80215-901, Department of Mechanical Engineering, Curitiba, Paraná, Brazil, Tel. 55 41 330-1346.
e-mail: ricardo@rla01.pucpr.br.

Wilson L. Guesser
Universidade Estadual de Santa Catarina, Tupy Fundições Ltda, Albano Schmidt St, 3400, Zip Code 89206-900, Joinville Santa Catarina, Brazil, Tel. 55 47 441-8359.
e-mail: wguesser@tupy.com.br.

(*) – This paper presents part of the results of the Master Thesis by Edvaldo C. Angelo Jr.

Abstract. In this work, ductile casting iron bars have been characterized by quantitative image analysis. The most important microstructure features in ductile iron are graphite nodules, pearlite and ferrite amount. The graphite nodules can vary in size, amount and nodularity. On the other hand, depending on the cooling rate the pearlite show a change in the lamellae distance. The main objective of this project is to apply the image analyses technique to characterize the microstructure of ductile casting iron produced by continuous casting. The microstructure features were determined in 50, 100 and 150mm diameter along the radius of the bars. It was observed that the nodule size and pearlite amount increases towards of bars core, on the other hand the number of nodules and the nodularity decrease. Due to the change in the bar diameter there is change in the fashion in which this microstructure feature changes from the surface to the core.

Keywords. *Quantitative Image Analysis, Ductile Iron, Continuous Casting.*

1. Introduction

The continuous castings process was developed as an alternative route for the production of cast iron without toolings normally used in conventional sand molding process. Due to the nature of the continuous casting process, typical defects found in conventional sand casting such as gas holes, centerline shrinkage and slag inclusion are not found in continuous casting products, according to FUCO® Manual (1998).

The continuous casting process makes possible the production of bars with fine grained as cast structure. The process consists on pouring the molten iron into a feeding furnace where a water-cooled graphite die gives the final shape and size of final cast components. In the continuous casting the water-cooled graphite die is mounted to the lower part of the feeding furnace leading the ferrostatic pressure that maintains the molten iron always passing through the die while a traction unit pulls the solidified bar horizontally as shown in Fig. (1).

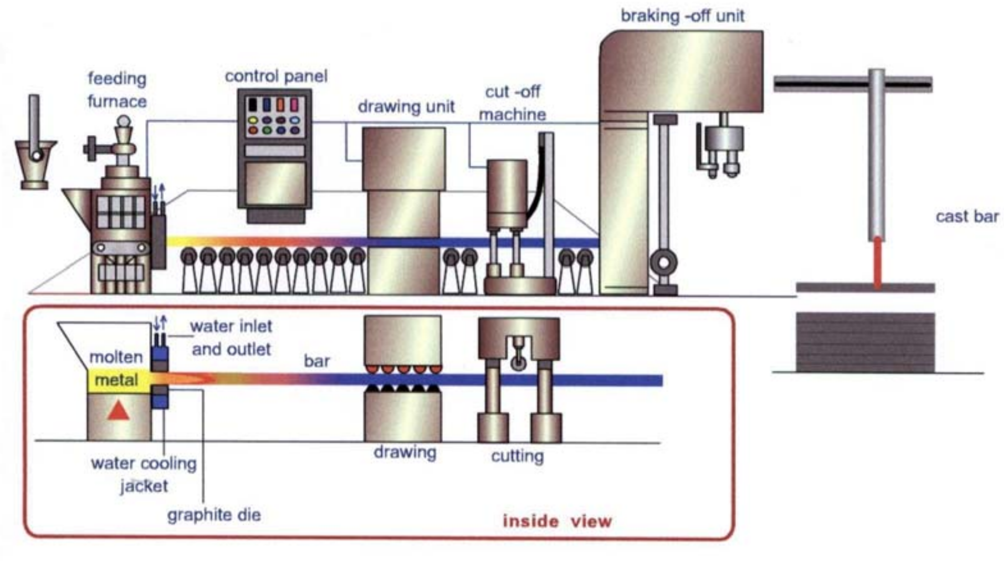

Figure 1. Continuous casting of cast iron bars.

Ductile Cast Iron is an alloy of iron, carbon and silicon. Carbon is added to the melt in amounts that exceed the quantity retained in the austenitic solid solution, forming graphite. Marks (1999) show that the graphite occurs in discrete spheroids or spherulites (each with a radial structure) distributed in an apparently random manner throughout the structure. Spheroidal graphite is produced by the addition of nodularizing elements, such as magnesium and cerium (often in combination with other rare earth elements). The tendency to form the graphite is regulated by the composition and the cooling rate. Graphite formation is promoted by the presence of silicon in concentrations greater than about 1% wt. Also, slower cooling rates during solidification and inoculation favors graphitization (the formation of graphite). The shape, the distribution and the size of graphite, as well as the structure of the matrix are important factors to determinate the casting mechanical properties. The determination of graphite shape, distribution and size, pearlite and ferrite are a crucial step to define the correct materials application. The main characteristic of the ductile iron grades is the spheroidal shaped graphite structure. The typical mechanical properties of ductile iron are leakage resistence, surface finish, toughness and ductility.

The materials behavior is a function of its microstructure. A given microstructure is a result of the chemical composition and the processing. The ability to determine the microstructure is an important parameter in manufacturing process control. The growing needs for accuracy and velocity in microstructure analyses brings the need for an automatic computerized technique. Image analysis is a technique for extracting quantitative data from images, usually with the objective to analyze the microstructure of the specimen, represented by the image. Viera et all (2001), show several benefits of automatic quantitative image analyses in comparison to traditional point counting, such as higher intrafield statistics for field measurements, faster data acquisition and the possibility to measure object parameters that are impossible to obtain through manual methods. The growing functionality of software along with microscope automation and digital image acquisition methods has led to a boom in the use of automatic image analysis for microstructural evaluation.

In ductile iron the transformation of austenite can proceed according to the stable or the metastable reaction. The reaction that provides a microstructure of graphite and ferrite is called stable and it is been represented in Eq. (1). The decomposition reaction of austenite in pearlite (ferrite and cementite) is called metastable and it is been represented in Eq. (2). The eutectoid transformation in ductile iron is characterized by a competitive process between the stable and metastable transformations. The stable reaction (forming ferrite and graphite), occurs at higher temperatures and, because of the difficulty of nucleation of graphite, it starts near the existing graphite particles (formed during the solidification). As the stable reaction proceeds, the diffusion distance (to transport carbon from austenite to the existing graphite particles) increases as shown in Fig. (2). On the other hand, the pearlite reaction is a cooperative transformation, due to the lamellar structure of pearlite, so it is a fast reaction and it can happen at high undercoolings. The pearlite reaction normally starts at intercellular areas (due to the concentration of pearlite promoting alloying elements), growing into the austenite as shown in Fig. (2). Figure 2 shows a sequence finishing with a matrix of ferrite and pearlite, with the two eutectoid reactions competing on the austenite decomposition.

$$\gamma \longrightarrow \alpha + Graphite \tag{1}$$

$$\gamma \longrightarrow \alpha + Fe_3C \tag{2}$$

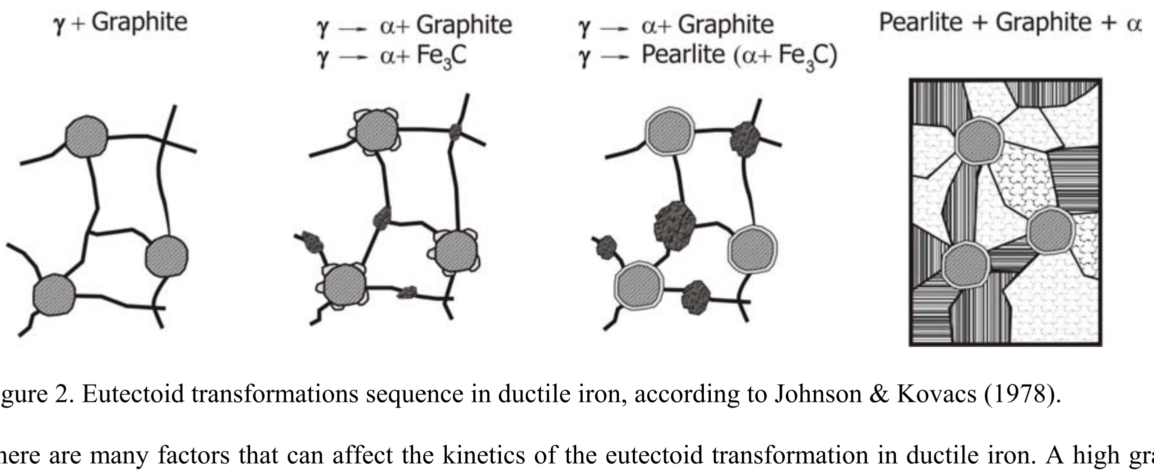

Figure 2. Eutectoid transformations sequence in ductile iron, according to Johnson & Kovacs (1978).

There are many factors that can affect the kinetics of the eutectoid transformation in ductile iron. A high graphite nodule number results in short carbon diffusion distances, so the ferrite formation is promoted. In the same way, low cooling rates in the eutectoid temperatures allows enough time for carbon diffusion, resulting in ferrite formation. On the other hand, low graphite nodule number and high cooling rates results in pearlite formation, according toGuesser and Ghisi Hilario (1999).

The graphite nodule number also depends on the cooling rate (during solidification), a high cooling rate resulting in high undercooling and, in this way, in a high graphite nucleation rate. So, at the surface of ductile iron bars, produced by continuous castings, one can expect a high nodule number (because of the high cooling rate). The result of the austenite decomposition depends on the competition of two factors: high nodule number (resulting in short distance for carbon diffusion, in this way promoting ferrite) and high cooling rate (leading to short time for diffusion, in this way promoting pearlite). In the different positions of the bar (mid radius, center) this competition will always be present and the matrix will be the result of that competition (nodule number effect and cooling rate effect).

Results from Askeland et all (1975) show that nodules count does have a pronounced effect on matrix structure, with a high nodule counts resulting in a highly ferritic matrix. However, at higher nodule counts the percent of pearlite decreases very little even with a considerable increase in nodule count.

In the same work Askeland et all (1975) shows that the amount of pearlite is very sensitive to changes in nodule count when the nodule count is low. Small changes in nodule count at the 100 nodules / mm^2 level give a large changes in percent of pearlite while changes of the same magnitude at the 600 nodules / mm^2 level produce little change in pearlite. This effect can be better understood by examinig the diffusion distances required for carbon atoms to diffuse to the graphite nodules, or by evaluating the interparticles spacing λ between the graphite nodules as show in Eq. (3). below.

$$\lambda = \left(\frac{2 \cdot \pi}{3 \cdot f} \right)^{\frac{1}{2}} \cdot r - \frac{\pi \cdot r}{2} \tag{3}$$

Where f is the volume fraction of graphite and r is the average radius of the nodules. If the nodules count were incresed from 100 to 200 nodules / mm^2, the interparticle spacing would be reduce by 50%. However, increasing the nodules count from 600 to 700 nodules / mm^2 would only reduce the interparticle spacing by 13%.

Table 1. Graphite Interparticle Spacings for Selected Nodule Counts, according to Askeland et all (1975).

Nodules/mm^2	Volume fraction of the graphite f	Average Radius of graphite (mm) r	Interparticle Spacing (mm) λ
99.3	0.125	0.0635	0.16
207	0.119	0.0317	0.08
616	0.147	0.0159	0.0375
706	0.161	0.0159	0.0325

The aim of this project is to evaluate the effects of nodule number and cooling rate on the matrix, applying image analyses techique to characterize the microstructure of ductile cast iron produced by continuous casting.

2. Experimental Procedures

In this work microstructural characterization was performed in continuous casting bars. The bars were produced in ductile iron according to ASTM A536 Class 65-45-12. In order to establish the effect of the cooling rate in the microstructure three bars with different diameters were produced by the continuous casting process.

The bars were sliced in eight samples as shown Fig. (3). The samples were polished for optical microscopy observation. For each 5 mm position in the samples eight randomly chosen fields were examined at 200x. The image analyses were performed according to ASTM A 247-67 using Image Pro-Plus of Media Cybernetics analyzer.

In each field the amount of pearlite and ferrite was determined as well as the microstructure features that concern the graphite nodule phase such as number, size and shape. The data were statistically treated and plotted as a function of the normalized distance. In the normalized distance the position zero corresponds to the surface of the bars, the position 0.5 corresponds to an intermediate position and the position 1 corresponds to the core of the bars.

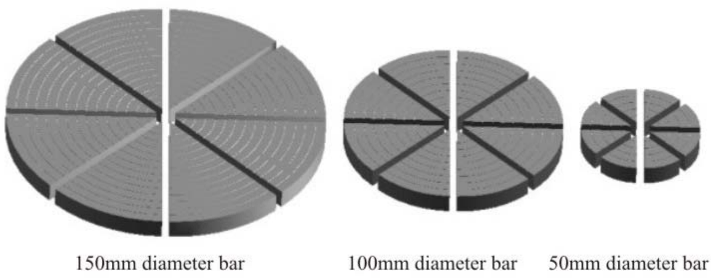

Figure 3. Continuous casting bars showing fashion that the samples were analyzed.

3. Results and Discussion

Number and size of graphite nodules, amount of pearlite and nodularity are shown in Fig. (4), Fig. (5) , Fig. (6) and Fig. (8) as a function of the normalized distance in the continuous casting bars.

The graphite nodule number decreases from the surface to the core of the continuous casting bars, illustrated in Fig. (4). The decay of the graphite nodules number is more dramatic for the 150 mm diameter. At a given position in the bars, the nodule number decreases with increasing the bar diameter. As a result of this trend, the size of the graphite nodules increases from the surface to the core of the bars as shown in Fig. (5). The results presented in Fig. (4) and Fig. (5) are in agreement because both microstructure features are carbon diffusion controlled. On the surface due to the higher cooling rate diffusion is very limited additionally the carbon finds a lower energy position without moving for very long distance resulting in large number of small nodules. On the core due to the slower cooling rate carbon diffuses for long distance resulting in a small number of large nodules.

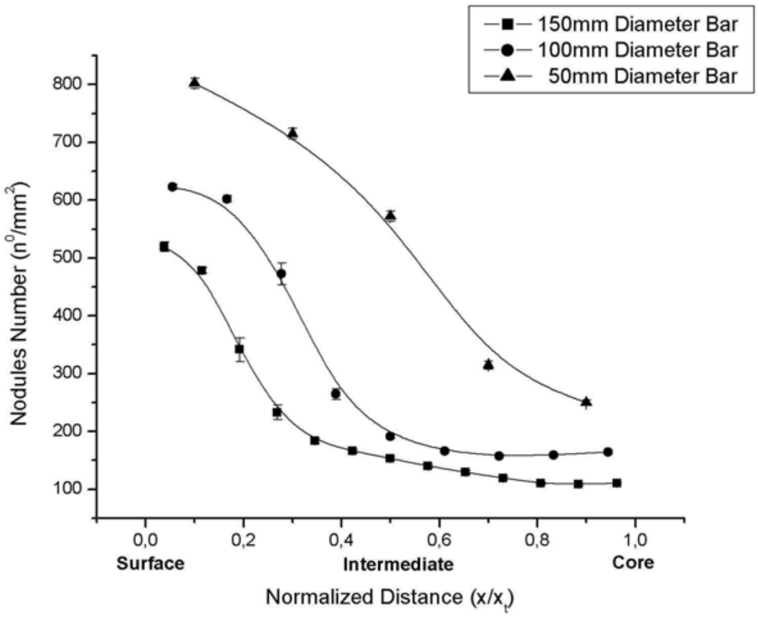

Figure 4. Graphite nodules number as function the normalized distance in the continuous casting bars.

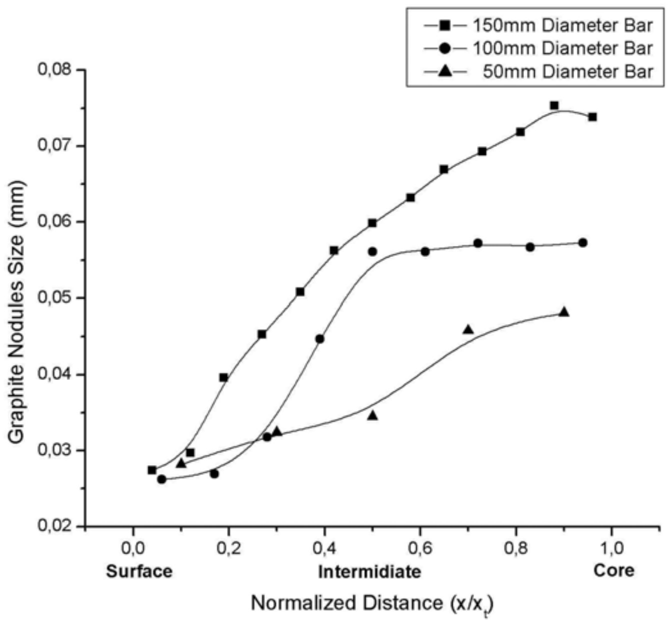

Figure 5. Graphite nodules size as function of the normalized distance in the continuous casting bars.

The amount of pearlite increases from the surface to core of continuous casting bars as shown in Fig. (6). At the 50 mm diameter bar, the variation of pearlite acroos the section is the opposite of the nodule number variation, as a result of high nodule number promoting ferrite formation by decreasing the carbon diffusion distance. On the other hand, for the 100mm and 150mm diameter bars the amount of pearlite show a maximum value in the intermediate position. A competitive process between the cooling rate and nodule number determine the amount of pearlite.

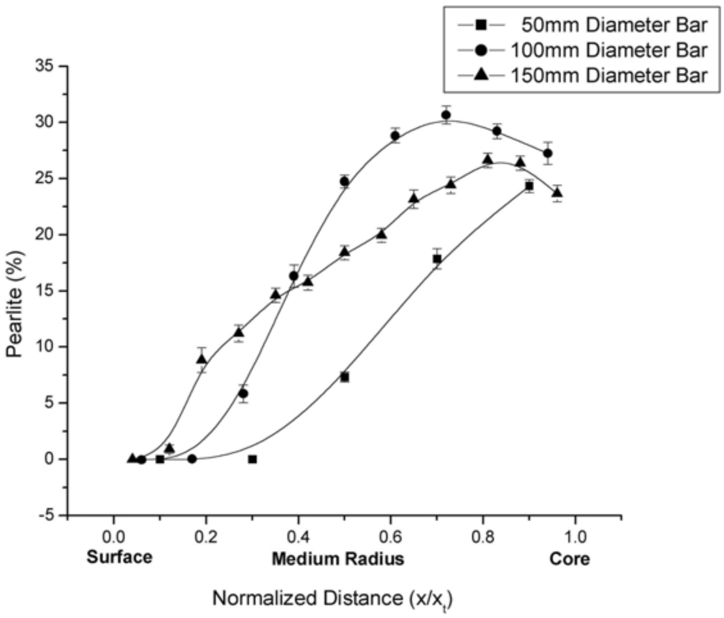

Figure 6. Amount of Pearlite as a function of the normalized distance in the continuous casting bars.

It is interesting to note that in all three bars there is a ferrite rim near the surface, as shown in Fig. (7). The water colled graphite die provide a higher cooling rate on the surface resulting in a large number of small nodules with a ferrite matrix.

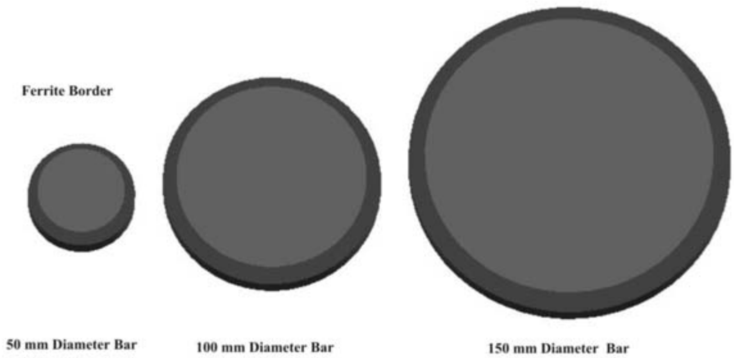

Figure 7. Ferritic rim of the continuous casting bars.

The nodularity is another important microstructure feature in ductile iron. Marwanga et all (2000) show that nodularity is thought to be a good indicator of the influence of graphite on machinability. It has been reported that increasing nodularity increases strength and elongation. In Fig. (8) the nodularity is plotted as a function of the normalized distance for the continuous casting bars. As can be noticed the nodularity is low on the surface. This tendency can be observed due to the process of decomposition of cementite above the eutectoid temperature as represented in Eq (4).

$$Fe_3C \longrightarrow \gamma + Graphite \tag{4}$$

In the 50mm diameter bar the nodularity shows its maximum in the position close to the mid radius while in the 100mm diameter bar the maximum in nodularity is observed close to the center. On the other hand the nodularity reaches a minimum at the center of the 150mm bar. Nodules count and nodularity is determined by the inoculation and nodularization treatment of the molten iron. The fading of magnesium and ferrosilicon lead to a low nodules count and low nodularity. At the center of the 150mm diameter bar longer solidification time leads to the fading of Mg and FeSi.

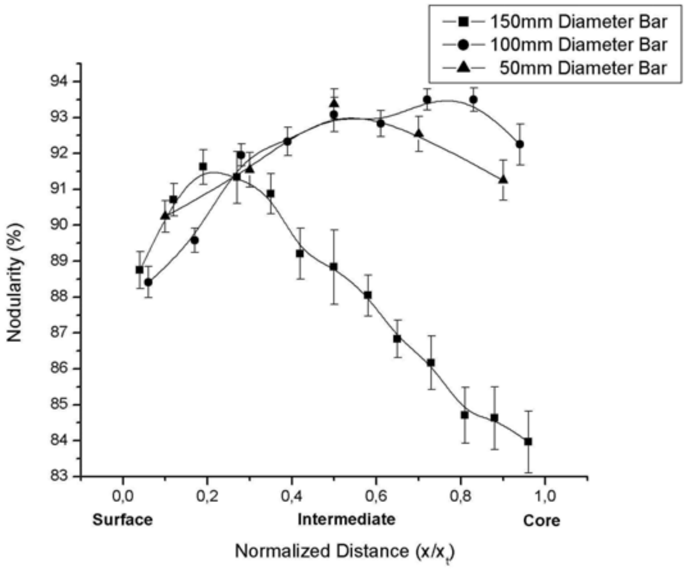

Figure 8. Nodularity as a function of the normalized distance in the continuous casting bars.

4. Conclusions

The microstructural gradiente has been determinated in ductile cast iron produced by continuous casting applying image analyses technique. This technique produces reliable results according to the metallurgical phase transformation.

The cooling rate is the major process parameter to be controlled in continuous casting in order to design an appropriate microstructure for a given application, although the influence of the cooling rate is much more pronouced at lower nodules count than at higher nodules count.

A ferritic rim is formed on the surface of the continuous casting bar as a result of the high cooling rate provided by the water-cooled graphite die.

There is a strong relation among nodule count and the amount of pearlite. On the surface of the bars the amount of pearlite is low because the nodule count is high. At the center or close to the center of the bar the amount of pearlite is high due to the low cooling rate and the low nodules count. The position of the maximum amount of pearlite depends on the bar diameter: for the 50 mm diameter bar, the maximum amount of pearlite happens at the center, while for the 100 mm and 150 mm diameter bars the position of this maximum amount of pearlite is observed at 0,7-0,8 of the radius.

The graphite nodules formed from the decomposition of cementite have lower nodularity than those formed from the liquid, as can be observed on the surface of the three diameter bars. Low nodularity can also be observed at the center of the bars, mainly on the 150 mm diameter bar, caused probably by the fading of Mg and inoculant.

5. References

Askeland, D.R., Gupta, S.S., 1975, “Effect of Nodule Count and Cooling Rate on the Matrix of Nodular Cast Iron” Transaction of the American Foundraymens´s Society, Vol. 83, pp. 313-320.

Brown, B.F., Hawkes, M.F., “Kinetics of Grafitization in Cast Iron”, Transaction of the American Foundraymens´s Society, Vol. 59, pp. 181-199.

FUCO® Manual Técnico, 1998, “Perfis de Fundição Contínua”, Indústria de Fundição Tupy.

Goodrich, G.M., 1993, “Ductile Iron Dilemma: Primary Carbides”, Modern Casting, Vol. 83, pp.48.

Guesser, W.L., Boehs, L., Carvalho Jr, D., Friedrich, D.N., 2000, “Usinabilidade de Perfis Contínuos de Ferros Fundidos Nodulares das Classes FE-45012 e FE-50007”, Sulmat.

Guesser, W.L. & Ghisi Hilario, D. “Ferros fundidos nodulares perlíticos”. CONAF-ABIFA, S Paulo, 1999.

Johnson, W.C. & Kovacs, B.V. The effect of additives on the eutectoid transformation of ductile iron**.** Metallurgical Transactions 9A :219-29, feb 1978.

Lalich, M.J., Loper Jr, C.R., 1973, “Describing the Eutectoid Transformation in Hyper-Eutectic Ductile Cast Iron”, Transaction of the American Foundraymens´s Society, Vol. 81, pp. 238-244.

Marks, J.R. “Metallography of Ductile Iron”, Transaction of the American Foundraymens´s Society, Vol. 107, pp. 819-827.

Marwanga, R.O., Voig, R.C. & Cohen, P.H., 2000, “Influence of Graphite Morphology and Matrix Structure on Chip Formation During Machining of Continuously Cast Ductile Iron”, Transaction of the American Foundrymen’s Society, Vol. 108, pp. 651-661.

Vieira, P.R.N., Paciornik, S., 2001, “Uncertainty Evaluation of Metallographic Measurements by Image Analysis and Thermodynamic Modeling”, Journal of Materials Characterization, Vol. 47, pp. 219-226.